Contents lists available at ScienceDirect

Carbohydrate Polymers

journal homepage: www.elsevier.com

Tuning rheology and aggregation behaviour of TEMPO-oxidised cellulose nanofibrils aqueous suspensions by addition of different acids

L. Alves [a, *], E. Ferraz [b, c], A.F. Lourenço [a], P.J. Ferreira [a], M.G. Rasteiro [a], J.A.F. Gamelas [a, *]

[a] CIEPQPF, Department of Chemical Engineering, University of Coimbra, Pólo II – R. Silvio Lima, 3030-790 Coimbra, Portugal
[b] Techn&Art, Polytechnic Institute of Tomar, Quinta do Contador, Estrada da Serra, PT - 2300-313 Tomar, Portugal
[c] Geobiotec, Geosciences Department, University of Aveiro, Campus Universitário de Santiago, PT - 3810-193 Aveiro, Portugal

ARTICLE INFO

Keywords:
Cellulose nanofibrils
Charged nanofibrils
Rheological properties
Hydrogels
Aggregation
Acids
Protonation
Hofmeister series

ABSTRACT

The present work intends to study the variations in the rheological properties and aggregation behaviour of TEMPO-oxidised cellulose nanofibrils (CNF) aqueous suspensions, as a function of changes in concentration and systematic changes in the pH, by addition of acids with different anions. It was found that CNF suspensions form strong gels at mass fractions higher than 0.35 % and the gel point is ca. 0.18 %. On the other hand, aggregation is enhanced at acidic pH conditions due to lower charge repulsion among fibrils, leading to an increase of the suspension viscosity. However, distinct rheological behaviours were presented by CNF suspensions as different acids were applied. It was found that phosphate ions resulted in significant aggregation leading to formation of particles of large size and very strong gels, at pH 2.3; distinctly, the presence of acetate ions resulted in lower aggregation, lower particle size and weaker gels, at the same pH value.

1. Introduction

Cellulose nanofibrils (CNF) are nanomaterials with high aspect ratio. Typically, TEMPO-oxidised CNF consist of long fibrils (up to 2 μm) with very low thickness (less than 10 nm) (Nechyporchuk, Belgacem, & Pignon, 2016). Derived from their high crystallinity and high aspect ratio, CNF suspensions form stiff hydrogels with high elasticity at a relatively low concentration (Jowkarderis & van de Ven, 2015). Thus, CNF suspensions appear as an interesting rheology modifier to be applied in cosmetics, paints, food, as mineral suspending agent, among other applications (Turbak, Snyder, & Sandberg, 1983). In addition, the excellent properties of the dried CNF materials, such as high stiffness and tensile strength, as well as low density and thermal expansion coefficient render this material in a good alternative to common plastics, to be applied in packaging applications or nanocomposites (Alves, Ferraz, & Gamelas, 2019; Henriksson, Berglund, Isaksson, Lindström, & Nishino, 2008; López-Rubio et al., 2007; Xie, Du, Yang, & Si, 2018).

CNF are obtained from wood pulp or non-woody resources by using appropriate chemical/enzymatic pre-treatments followed by mechanical treatment. TEMPO-oxidised CNF are prepared by first treating cellulose pulp with sodium hypochlorite in the presence of catalytic amounts of TEMPO (2,2,6,6-tetramethylpiperidine-1-oxyl radical) and sodium bromide, followed by mechanical homogenisation of the oxidised fibres suspension (Lourenço et al., 2017). It is known that charge density and fibril dimensions directly affect the suspension rheology (Jowkarderis & van de Ven, 2015). The CNF preparation with TEMPO introduces charges along the nanofibrils surface by oxidation of OH groups. The resultant CNF suspensions consist in strong gels at relatively low consistency levels, of less than 1%, due to the formation of highly entangled networks. Compared to other CNF preparation methods, such as enzymatic or only mechanical, TEMPO-oxidised fibrils form stronger gels, due to higher fibrillation degree, higher fibril stiffness and better aqueous dispersion.

* Corresponding authors.
Email addresses: luisalves@ci.uc.pt (L. Alves); jafgas@eq.uc.pt (J.A.F. Gamelas)

https://doi.org/10.1016/j.carbpol.2020.116109
Received 14 November 2019; Received in revised form 27 February 2020; Accepted 2 March 2020
Available online xxx
0144-8617/

Suspensions of cellulose nanofibrils obtained from TEMPO-oxidised fibres are typically highly viscous, which can compromise or difficult some applications. Rheology of polymeric suspensions is controlled by physical entanglement of the chains and aggregation (Alves et al., 2015). Similarly, viscosity of CNF suspensions is controlled by entanglement of cellulose nanofibrils and its aggregation, being possible to tune the suspension properties by changing some conditions such as concentration, pH, ionic strength or added co-solutes (Fukuzumi, Tanaka, Saito, & Isogai, 2014; Hubbe et al., 2017; Sato, Kusaka, & Kobayashi, 2017).

These phenomena can thus be used to control suspension's viscosity and stiffness, being possible to induce bridging and flocculation of negatively charged fibrils by addition of polyelectrolytes, di- or trivalent salts or by decreasing pH to acidic values (Sato et al., 2017). Besides the rheological control, aggregation can be used to increase dewatering of CNF suspensions, mainly suspensions of charged fibrils, in which the dewatering process is usually complicated and compromises the application of this kind of fibril suspensions in papermaking (Jowkarderis & van de Ven, 2015) or in the preparation of films by filtration. CNF films prepared by filtration, followed by hot pressing or oven drying, appear as an interesting option compared with solvent casting due to time saving and improved mechanical properties obtained by this method (Alves et al., 2019).

In literature it is possible to find works reporting rheological and aggregation studies of TEMPO-oxidised cellulose nanofibrils suspensions (Calabrese et al., 2019; da Silva et al., 2018; Dimic-Misic, Maloney, & Gane, 2018; Fukuzumi et al., 2014; Lasseuguette, Roux, & Nishiyama, 2008; Mendoza, Gunawardhana, Batchelor, & Garnier, 2018; Moberg et al., 2017; Quennouz, Hashmi, Choi, Kim, & Osuji, 2016; Sato et al., 2017; Šebenik, Krajnc, Alič, & Lapasin, 2019). As examples, the effects of fibril length, aspect ratio and surface charge on shear-induced structuring in TEMPO CNF aqueous suspensions and other gels rheological properties were evaluated by Moberg et al., Dimic-Misic et al. and Mendonza et al. (Dimic-Misic et al., 2018; Mendoza et al., 2018; Moberg et al., 2017). Fukuzumi et al. presented a work dealing with dispersion stability and aggregation behaviour of TEMPO-oxidised cellulose nanofibrils in water as a function of salt addition (Fukuzumi et al., 2014). Šebenik et al. studied the ageing effect of aqueous TEMPO-oxidised CNF dispersions prepared from commercially available TEMPO CNF powder (Šebenik et al., 2019). The heat driven gelation was studied by Calabrese et al. (Calabrese et al., 2019). Other examples are the works of da Silva et al. who reported the gelation of TEMPO-oxidised nanofibril dispersions induced by addition of alcohol (da Silva et al., 2018) and Quennouz et al. who presented a rheological study of cellulose nanofibrils in the presence of surfactants (Quennouz et al., 2016). On the other hand, Sato et al. reported the charging and aggregation behaviour of TEMPO CNF in aqueous solution by means of light scattering studies, atomic force microscopy and electrophoresis (Sato et al., 2017). Additionally, Schenker et al. studied the influence of the degree of fibrillation and residual fibre content on flow and viscoelastic properties of microfibrillated cellulose (Schenker, Schoelkopf, Gane, & Mangin, 2019). However, the effect on aggregation and rheological behaviour of pH decrease induced by the addition of acids of different nature was not explored.

The present study reports the rheological behaviour of suspensions of TEMPO CNF as function of nanofibrils concentration and suspension pH, the latter effect evaluated by addition of different acids (acetic, lactic, citric and phosphoric). As one of the potential applications of the CNF is in films for food packaging, the acids chosen to change pH of the suspension were food additive compounds, all used in food industry to avoid possible contamination of food, after packaging, with hazardous compounds. The rheometry and dynamic light scattering results showed significant differences in shear viscosity, apparent yield stress and particle size, at the same pH value, as different acids were used.

2. Materials and methods

2.1. Chemicals

In this study the following acids were used: acetic acid (ACS Reag. Ph. Eur., > 99.9 %); lactic acid (AnalaR NORMAPUR, > 89.2 % in aqueous solution); phosphoric acid (USP-NF, Ph. Eur., 85 % in aqueous solution); and citric acid (> 99.5 %). All the reagents were obtained from VWR International and used without any further purification.

2.2. Nanofibrils preparation and characterization

The cellulose nanofibrils were produced from an industrial never dried bleached *Eucalyptus globulus* kraft pulp, as reported elsewhere (Lourenço et al., 2017). The cellulose fibres were firstly refined at 4000 rev. in a PFI beater. Afterwards, the fibres were oxidised with NaClO using a ratio of 7 mmol of NaClO per g of dry pulp and catalytic amounts of TEMPO and NaBr, according to a methodology developed by Saito et al. (Saito, Kimura, Nishiyama, & Isogai, 2007). The oxidised fibres were filtered and washed thoroughly with distilled water. Finally, the fibres were mechanically treated in a high-pressure homogenizer (GEA Niro Soavi, model Panther NS3006 L), firstly at 500 bar and secondly at 400 bar.

The yield of nanofibrillation was determined in duplicate after centrifugation of a CNF aqueous suspension (0.2 wt%) at 9000 rpm for 30 min. The carboxyl content was determined in duplicate by conductometric titration of the aqueous suspension of CNF (acidified to pH of ca. 3) with NaOH 0.01 M. The degree of substitution (DS) by carboxyl groups of the CNF was estimated from the CNF carboxyl content. Intrinsic viscosity measurements were performed in the CNF suspension by dissolving it in cupriethylenediamine, according to the ISO standard 5351:2010. The degree of polymerization (DP) was then calculated using the Mark-Houwink equation, with parameters $K = 0.42$, $a = 1$ (Henriksson et al., 2008).

A CNF aqueous gel with 0.77 wt% of dry content was obtained. The yield of nanofibrillation was found to be close to 100 % (no phase's separation was detected after centrifugation). The determined carboxyl content was 1.41 mmol g^{-1} (DS = 0.23), intrinsic viscosity was 153 ml g^{-1}, and the DP estimated from the intrinsic viscosity results was 365.

2.3. Rheology and aggregation studies of nanofibrils suspensions

2.3.1. Nanofibrils suspensions preparation

The TEMPO CNF suspensions for analysis were prepared by dilution of the original suspension of nanofibrils (0.77 wt%), by weighing the desired amount of suspension and adding the required mass of distilled water. Solutions were kept under stirring during 30 min to ensure a good dispersion of the fibrils. 0.5 M stock solutions of the different acids were prepared to be used for pH adjustment. After acid addition all the samples were left to equilibrate during 30 min under agitation and pH was measured after this period.

2.3.2. Rheology

Rheological measurements were performed at constant temperature (25 °C) in a controlled stress rheometer (Model RS1, Haake,

Germany) using a cone-plate geometry (C60/1) for the rotational tests and a plate-plate geometry (PP20Ti) for the oscillatory tests, connected to a temperature control recirculation bath (Haake Phoenix II, Germany). Flow curves were obtained in controlled stress mode applying shear stresses ranging between 1.0 and 50.0 Pa. The complex viscosity, storage modulus (G') and loss modulus (G") were accessed by performing dynamic oscillatory experiments from 10 to 0.01 Hz. The power law parameters, fitted using the Ostwald-de Waele model, were obtained using the Haake Rheowin 4.20.005 software (Haake, Germany).

2.3.3. Polarised light microscopy

An Olympus BH-2 KPA microscope (Olympus Optical Co., Ltd, Japan) equipped with a high-resolution CCD colour camera (Olympus ColorView III) was used to observe the cellulose nanofibril samples, at different pH values and a consistency of 0.09 %. Samples were kept between cover slips and illuminated with linearly polarised light and analysed through a crossed polarizer. Images were captured and analysed using the analySIS software (Soft Imaging System GmbH).

2.3.4. Dynamic light scattering and zeta potential

Dynamic light scattering (DLS) measurements were used to estimate the particle size of the cellulose nanofibrils. Measurements were performed in a Zetasizer NanoZS equipment (ZN 3500, Malvern Instruments, UK), with a 532 nm laser, using a backscatter angle detection of 173°, at 25 °C. CNF suspensions with a concentration of 0.05 wt% were centrifuged at 4000 rpm for 10 min, previously to pH adjustment and size measurements in order to remove large particles in suspension. The concentration of the suspensions used was lower than the estimated overlap concentration to avoid extensive interactions among fibrils. The suspensions were then gently transferred to a glass cuvette and checked for the presence of bubbles. The average particle size was determined, based in six repetitions, using the Zetasizer Nano Software (version 7.11). The data were analysed according to the non-negative least-squares (NNLS) algorithm.

Zeta potential measurements were carried out in the same equipment and with the same software, by electrophoretic light scattering, based in six repetitions to each sample.

3. Results and discussion

Polymeric solutions usually present shear thinning behaviour. Cellulose nanofibrils suspensions typically behave as polymeric solutions, forming an entangled network above a critical concentration, being that network destroyed by increasing shear forces, leading to viscosity decrease (Vadodaria, Onyianta, & Sun, 2018). Fig. 1 shows the flow curves obtained for TEMPO-oxidised CNF for different fibrils concentrations.

An increase in the apparent shear viscosity of the suspensions as the concentration increases could be observed. To low shear rates, suspensions containing a CNF mass fraction higher than 0.18 % presented high viscosities, due to the presence of the entangled network. The suspension containing the lowest mass fraction, 0.09 %, behaved differently due to the absence of an entangled network that only occurs above a specific concentration, named overlap concentration; for the present CNF suspensions the overlap concentration is between 0.09 and 0.18 %, as can be seen in Fig. 1.

The increase of the CNF mass fraction can also lead to gel formation. Fig. 2 shows the oscillatory tests performed on nanofibrils suspensions as function of frequency, for different fibrils mass fractions.

The suspension containing 0.09 % of CNF presented a G'' value higher than G', in the studied frequency range, i.e., liquid-like behaviour. At mass fraction of 0.18 %, G' and G'' values were similar, with the G' value only slightly higher, implying that the elastic properties are equivalent to the viscous properties, thus being close to the estimated gelation point for the present TEMPO-oxidised nanofibrils. The obtained results are in line with values previously reported in literature. For example, values of mass fraction of 0.15 % were reported as the gelation point of TEMPO CNF with a surface charge of 0.65 meq g^{-1} (Jowkarderis & van de Ven, 2015), about half of the charge of the nanofibrils used in the present work (1.41 mmol g^{-1}); the higher charge of the latter CNF explains the slightly higher gel point value obtained due to higher interfibril repulsion. For higher fibrils concentrations, the elastic modulus (G') was higher than the viscous modulus (G''), indicating a solid-like behaviour, being observed a considerable increase in G' modulus upon increasing the fibrils concentration.

Besides entanglements, aggregation also plays a major role on the suspension rheology behaviour (da Silva et al., 2018). Aggregation of negatively charged fibrils can be promoted by, e.g., reducing surface charge density by carboxyl groups protonation (Hubbe et al., 2017; Sato et al., 2017), salt addition (Fukuzumi et al., 2014), addition of oppositely charged molecules (Jowkarderis & van de Ven, 2015) or by changing the solvent polarity (da Silva et al., 2018). Fig. 3 shows the flow curves obtained for 0.35 % TEMPO CNF suspensions at different pH values, with the pH adjusted with acetic acid.

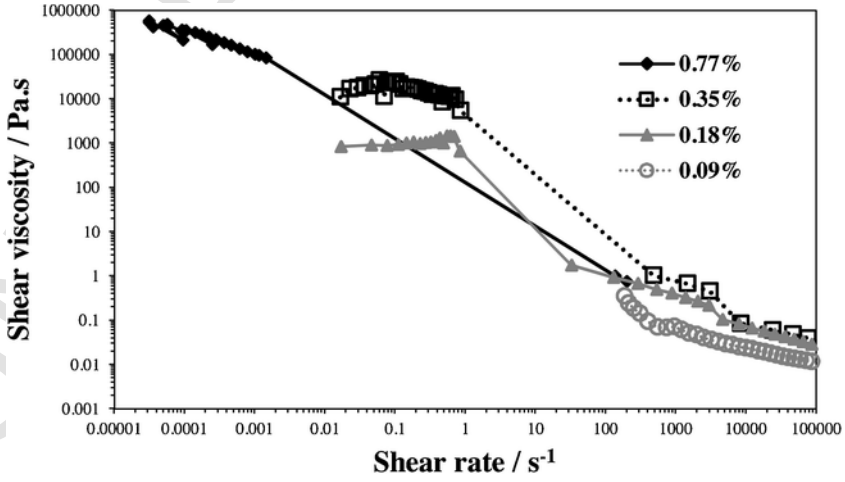

Fig. 1. Flow curves (with apparent shear viscosity) of TEMPO CNF aqueous suspensions as function of shear rate, at constant temperature (25 °C).

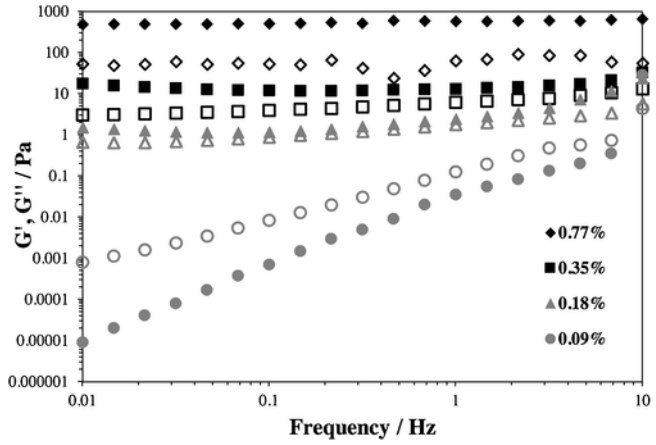

Fig. 2. G' (solid symbols) and G'' (open symbols) of TEMPO CNF suspensions as function of frequency, at 25 °C.

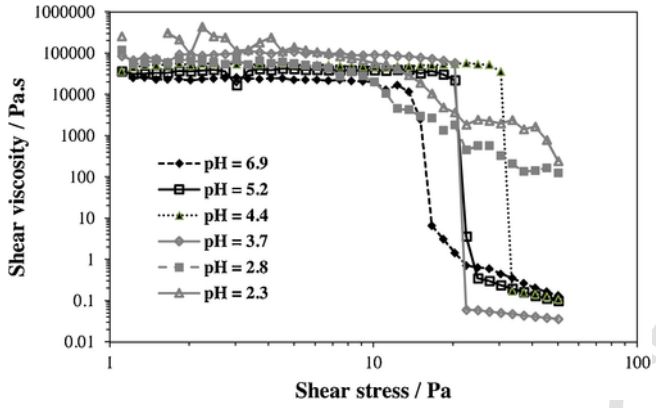

Fig. 3. Flow curves (with apparent shear viscosity) of TEMPO CNF aqueous suspensions (0.35 % CNF) as function of shear stress, at different pH values, adjusted with acetic acid, at 25 °C.

The suspension at pH 6.9 showed high apparent viscosity (ca. 30,000 Pa.s) at low shear stress values and is a relatively strong gel (Fig. 2). As the pH is decreased the trend is to increase the apparent viscosity values, at low shear values. At pH 2.3, the suspension presented the highest apparent viscosity values, of ca. 200,000 Pa.s (at low shear stress). As the shear stress values increase it was possible to see a fast decrease in apparent viscosity values due to the disentanglement of fibrils and consequent alignment induced by flow, once a certain value of shear stress is achieved; for the suspensions adjusted to lower pH values, i.e. pH 2.8 and 2.3, the apparent viscosity drop was less pronounced due to a higher fibrils aggregation. Similar trends were observed for the CNF suspensions where lactic, citric and phosphoric acids were used (See figure S1 in supplementary material).

The stress that must be applied to the sample before it starts to flow, i.e. disrupt the network, is the yield stress point. This value can be obtained from flow curves or from oscillation amplitude sweep tests (cross-over of G'/G''). The changes in the structure of fibrils suspensions are given by the oscillatory stress dependence of the phase angle (δ), which describes the phase lag between the viscous and elastic components of the complex modulus, where:

$$\tan\delta = \frac{G''}{G'} \quad (1)$$

Values of δ above 45° indicate tan δ > 1 and G" > G' (predominantly viscous behaviour) while values of δ below 45° indicate G' > G" (predominantly elastic behaviour) and δ = 45° indicates the phase transition (G'' = G').

Fig. 4 shows the apparent yield point results obtained for suspensions with 0.35 % CNF, at pH 4.4, with pH adjustment using different acids, where the fibrils present a charge density slightly inferior to 50 % of the charge achieved by complete ionization of the carboxyl groups (pK_a of $COOH/COO^-$ is 4.8 (Wågberg et al., 2008)).

The apparent yield point obtained for the original CNF suspension at neutral pH was ca. 15 Pa. Similarly, at pH 4.4, with pH adjustment done with lactic and citric acid the values obtained were close to that at the neutral pH, ca. 19 Pa (citric acid) and ca. 13 Pa (lactic acid). On the other hand, when acetic or phosphoric acid were used the apparent yield stress increased to ca. 24 Pa (acetic acid) and 26 Pa (phosphoric acid). The values obtained from oscillation amplitude sweep tests are in reasonable agreement with the values obtained from the flow curves of the same suspensions (see figure S2 for yield stress determination from flow curves).

Fig. 5 shows the changes in the phase angle (from the mechanical spectra) of 0.35 % CNF suspensions adjusted at pH 2.3 with four different acids.

The results obtained by acetic acid adjustment were quite different compared to those of the other acids used. In the studied oscillatory stress range, no change in behaviour was observed for suspensions adjusted with phosphoric, citric and lactic acids; contrary, when acetic acid was used, a transition from solid-like to liquid-like was obtained at ca. 78 Pa (see figure S3 for mechanical

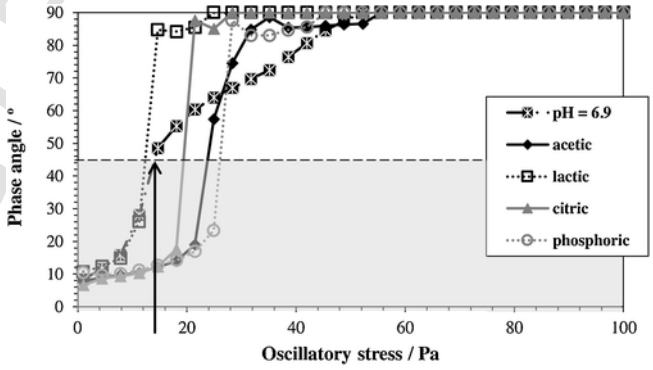

Fig. 4. Changes in phase angle of TEMPO CNF aqueous suspensions (0.35 % CNF), at pH 4.4, as function of oscillatory stress (at 1 Hz) for the different acids added, at 25 °C. Results of the initial suspension at pH 6.9 are also shown for comparison and the arrow indicates the apparent yield stress of this suspension.

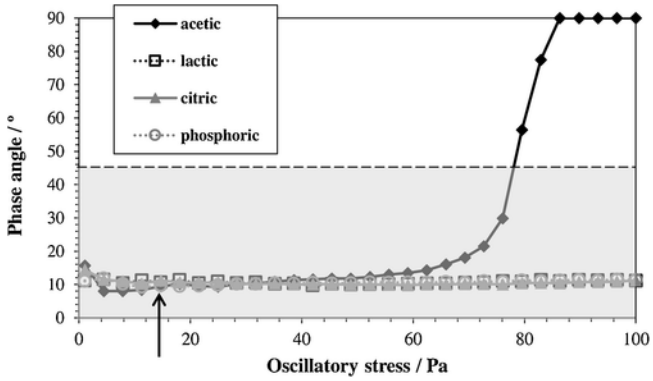

Fig. 5. Changes in phase angle of TEMPO CNF aqueous suspensions (0.35 % CNF), at pH 2.3, as function of oscillatory stress (at 1 Hz) for the different acids added, at 25 °C. The arrow indicates the apparent yield stress of the initial suspension at pH 6.9.

spectra). This means that at pH 2.3, the network formed when acetic acid is used is weaker than when the other studied acids are used, presenting a yield stress point lower than with the other acids (with phosphoric, citric and lactic acid the yield stress point is certainly higher than 100 Pa). At pH 2.3, the charge density of CNF is very low, being most of the carboxylic group's protonated. Thus, aggregation is expected for these suspensions, leading to a viscosity increase and shifting of yield stress to higher values. However, comparing the four different acids used, it is possible to predict differences in aggregation due to the significant differences obtained in rheological measurements. Rotational tests applied to the same CNF samples at pH 2.3, in the shear stress range between 1 and 50 Pa, demonstrated that the suspensions roughly follow the power law or Ostwald–de Waele model (Eq. 2) in the measured shear rate range,

$$\sigma = \mathrm{K} \times \dot{\gamma}^{n} \quad (2)$$

where K is the consistency coefficient, and n is the flow behaviour index. A n equal to unity indicates a Newtonian fluid. Non-Newtonian fluids are expressed by n values smaller than 1, indicating a pseudo-plastic (or shear thinning) behaviour, whereas n higher than 1, indicates a dilatant (or shear thickening) behaviour. Table 1 summarizes the values obtained for the power law parameters of the different suspensions and Figure S4 shows the fittings of the experimental data to the Ostwald–de Waele model.

Table 1
Power law parameters for TEMPO CNF suspensions (0.35 %) at different pH values adjusted with distinct acids.

Acid type	pH	K (Pa s^n)	n	R
Acetic	4.4	1.37×10^4	0.840	0.979
Lactic		3.14×10^4	0.942	0.995
Citric		0.95×10^4	0.808	0.985
Phosphoric		1.28×10^4	0.818	0.994
Acetic	2.3	8.72×10^1	0.262	0.980
Lactic		4.25×10^5	0.926	0.990
Citric		6.96×10^5	0.953	0.988
Phosphoric		3.59×10^5	0.919	0.986

The fitting parameters and the correlation coefficients (R) were obtained using the Haake Rheowin 4.20.005 software.

As can be seen, the parameters obtained at pH 4.4 for consistency and flow indexes were quite similar for the different acids used, with a slight increase observed with lactic acid. On the other hand, at pH 2.3, the suspension adjusted with acetic acid presented a quite different consistency index and also a smaller flow index compared with the suspensions adjusted with the other acids. This means that the viscosity of this suspension is more affected by the stress applied than the suspensions adjusted with the other acids, where the viscosity, although not constant, does not change much in the shear stress range studied (n is approximately 1). The differences observed can be related with different aggregation behaviour induced by the differentiated interaction of the acids anions with the fibrils, which can significantly change the aggregation extension and consequently the rheological properties of the suspensions. Aggregated fibrils can act to reinforce the formed network leading to a viscosity increment due to particle size growth. Our results showed a trend comparable to that observed in studies using a synthetic pH sensitive hydrophobically modified polymer, in which it was demonstrated that swollen particles lead to high viscosity increment and gelation of polymer suspensions, due to the increase in polymer particle size and volume occupied by particles (Alves et al., 2014, 2015).

In order to study the fibrils aggregation, optical microscopy and dynamic light scattering were used. The results obtained for the microscopic studies, particle size and zeta potential are presented in Figs. 6 and 7.

Images obtained by optical microscopy, under polarised light, showed the absence of large particles, including fibril aggregates, for a suspension at pH 6.9 containing 0.09 % (mass fraction) of CNF. As the pH is decreased to 2.3, the aggregation of fibrils is no-

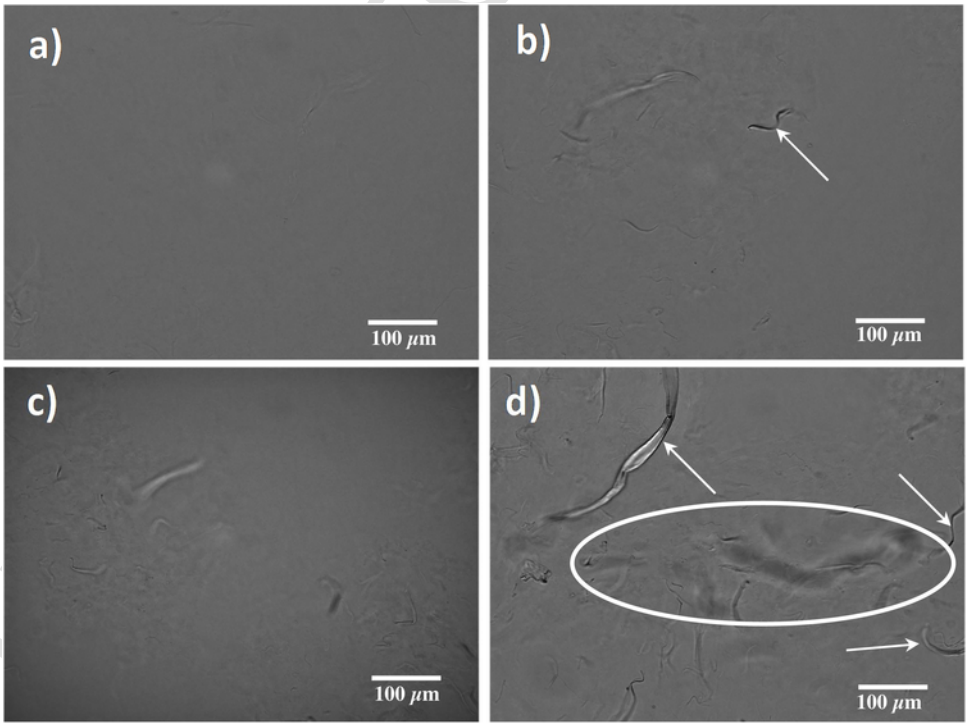

Fig. 6. Polarised light microscopy images of suspensions containing 0.09 % TEMPO CNF, at 25 °C. a) pH = 6.9; b) after pH adjustment to 2.3 with acetic acid; c) pH = 2.3 adjusted with citric acid; d) pH = 2.3 adjusted with phosphoric acid.

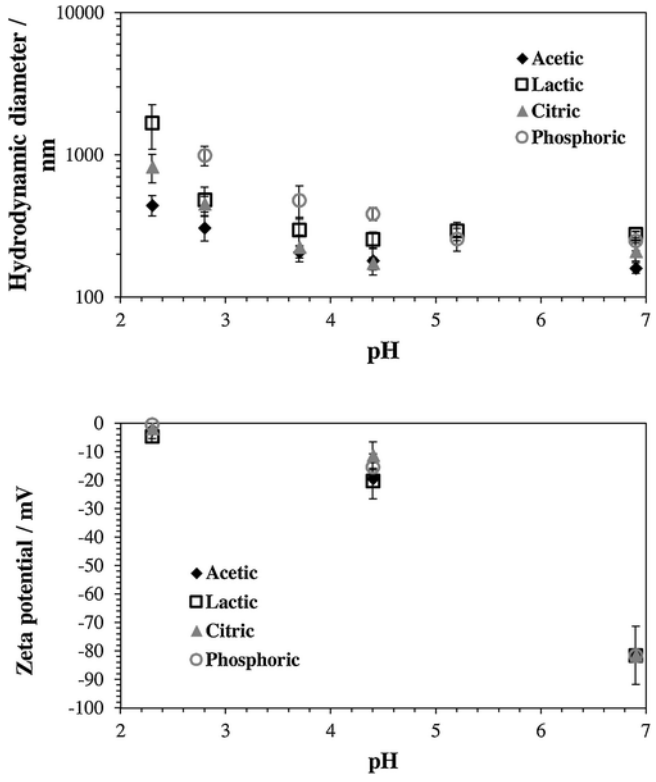

Fig. 7. Hydrodynamic particle size (Di0.5) obtained by dynamic light scattering (intensity-weighted distribution) (top) and zeta potential (bottom) for TEMPO CNF suspensions (0.05 %), at 25 °C, in the pH range between 6.9 and 2.3, pH having been adjusted with different acids.

ticed leading to the appearance of very large bundles of fibrils (several hundred microns). Also, some fibres of cellulose appeared in images being probably trapped by the growth of the aggregates (arrows indicate some of these cellulose fibres). In line with the rheology studies, the sample of CNF and acetic acid presented a clearer image compared to the other acids, indicating the presence of less fibril aggregates and of lower size. The results obtained by dynamic light scattering showed a similar trend, as described below, Fig. 7, top.

As can be seen, as the pH is decreased the average hydrodynamic particle size tendentiously increases, as expected due to the reduction of the amount of charged carboxylic groups and consequent reduction in counterion entropy and electrostatic repulsion among fibrils. However, very distinct behaviour was observed according to the acid used to adjust pH of the fibril suspensions. In the pH range from 6.9 to 4.4, the particle size changes were negligible. At pH 4.4, the particle size of the fibril suspensions started to differ depending on the acid used. For the suspensions adjusted with lactic, citric or acetic acids only slight changes were observed, within the experimental uncertainty. Different trend was observed for the adjustment using phosphoric acid, with a particle size increase of ca. 50 %. These results are in line with the yield stress values obtained at pH 4.4, in which the value obtained for the cellulose fibrils suspension adjusted with phosphoric acid presented the highest increase, ca. 11 Pa, compared to that of the suspension at pH 6.9 (Fig. 4).

When the suspension pH is decreased to 2.3 the size increment is much more pronounced. The suspension adjusted with acetic acid suffered aggregation as shown by the increase of more than 175 % (from 160 nm to 445 nm), being the lowest increment observed. In the case of citric acid adjustment, the particle size growth was more pronounced with a particle size increment of nearly 300 %, from ca. 210 nm–820 nm. With the lactic acid at pH 2.3 the average particle size was even higher when compared with the former acids, being observed a size growth of ca. 500 %. Following the trend observed at pH 4.4, the adjustment made with phosphoric acid led to the formation of aggregates of very large size, being not possible the size measurement using dynamic light scattering, because of the existence of two decay rates (showing the existence of two different hydrodynamic diameters), and low or inexistent correlation, indicative of the presence of particles with dimensions out of the range of dynamic light scattering application (see figures S5 and S6 for the correlation functions).

The results obtained for particle size are in good agreement with the ones reported by Sato et al. who studied the charging and aggregation behaviour of CNF in aqueous solutions as function of pH (Sato et al., 2017). Authors investigated the aggregation behaviour at different ionic strengths as function of pH (adjusted with HCl) and found a significant particle size increase for pH values below 4, more pronounced at the ionic strengths of 50 and 100 mM (KCl). At higher ionic strengths, the size increase with pH reduction became less relevant, due to extensive charge screening as a result of high salt concentration in solution.

The zeta potential results (Fig. 7, bottom) show a reduction in zeta potential as pH is decreased, being this drop more pronounced in the pH range from 6.9 to 4.4, where the pH corresponding to the pK_a of carboxylic groups (ca. 4.8 (Wågberg et al., 2008)) appears. It is easily calculated that for a pH value one point higher than pK_a (5.8 in the present case) ca. 90 % of carboxylic groups are deprotonated, and for a pH value one point lower than pK_a (3.8 in the present case) ca. 90 % are protonated (Reijenga, van Hoof, van Loon, & Teunissen, 2013). In the pH range of 4.4 to 2.3, the decrease of zeta potential was less pronounced also due to the low charge density already present on the CNF surface. At pH 4.4, the zeta potential of the CNF suspensions varied between -11.0 and -20.0 mV, the lower potential (in absolute value) having been obtained when citric acid is used, and the higher with lactic and acetic acids. At pH 2.3, all the cellulose fibrils presented a very low zeta potential due to almost full protonation of the carboxylic groups. Mautner et al. reported for TEMPO CNF the isoelectric point to be at a pH of 1.5 (Mautner, Hakalahti, Rissanen, & Tammelin, 2018). However, the value obtained in the present study for the suspension adjusted with phosphoric acid was ca. pH 2.3. Being expected an identical protonation to a specific pH value, independent of the acid used, the differences in particle size and zeta potential can be explained by differences in the electrical double layer (Sato et al., 2017), according to the acid used.

Looking to the partition coefficients of the used acids it is possible to notice significant differences. The Log P values range from -0.31 (at 20 °C) for acetic acid (Sangster, 1989) until -1.65 (20 °C) for citric acid (Kubáň, 1991), being -0.62 for lactic acid (Collander, 1951). Phosphoric acid is highly water soluble and thus the partition coefficient is not available in literature; however, this acid is clearly more hydrophilic than the other three tested. About the effect of these acids in solubility/insolubility of cellulose nanofibrils it is possible to rationalize the effect of the anions looking to salting-in/salting-out effect (Hofmeister series). Ions like phosphate are very water soluble and a poor affinity with virtually neutral fibrils (carboxylic groups almost fully protonated) is expected; on the other hand, a better interaction is expected for ions as acetate, due to its lower water solubility. The presence of acetate anions close to fibrils surface can stabilize the particles and reduce aggregation but this behaviour is not expected for phosphate anions. Consequently, higher aggregation is observed for CNF suspensions containing phosphate ions (higher salting-out effect) while acetate induces lower aggregation (salting-out effect

less pronounced). The salting-in and salting-out effects are very well described for interactions of cations and anions with proteins (Okur et al., 2017) and similar trends were observed for interactions with non-ionic polymers (Joshi, 2011) and other biopolymers (Mráček et al., 2008).

4. Conclusions

The present work explores the effects of different acids on the rheology and aggregation behaviour of TEMPO cellulose nanofibrils (CNF). The estimated gelation point of the fibrils suspensions used in the present study was ca. 0.18 % (at pH 6.9), being the overlap concentration between 0.09 % and 0.18 %. For concentrations above 0.18 %, the suspensions behaved as a solid, being the gel strength increased by an increment in fibrils concentration, due to the increment in physical entanglements and reinforcement of the network. Besides entanglements, fibrils aggregation also plays a major role in the rheology of the suspensions. With the decrease of pH and concomitant protonation of carboxylic groups, the suspension's viscosity increased. This effect resulted from the fibrils aggregation due to the decrease in charge repulsion among fibrils; however, the charge reduction in the fibrils also led to a weakening of the network stiffness and consequently to a faster network disruption, shifting the shear thinning to lower shear rate values.

The anion of the acid used to adjust the pH of suspensions was found to have an important effect on fibrils aggregation and consequently on rheology of the suspensions. Acetate ions led to lower aggregation of TEMPO CNF fibrils when compared to phosphate, lactate or citrate ions. In particular, phosphate anions resulted in an extensive aggregation of fibrils. As a consequence, the CNF suspensions adjusted with phosphoric acid presented higher yield stress values and formed stronger gels at low pH. Accordingly, large aggregates were observed by optical microscopy (at pH 2.3) and the dynamic light scattering study also revealed larger particles, when comparing to the use of the other acids. These distinct behaviours could be explained by differences in the interactions of the anions with virtually neutral fibrils, following the Hofmeister series. Thus, the use of different acids to control the suspension pH appears as an interesting tool to tune rheology of TEMPO CNF suspensions and can be also useful to improve dewatering of this type of suspensions, being phosphoric acid the most promising compound for this task.

CRediT authorship contribution statement

L. Alves: Conceptualization, Investigation, Methodology, Writing - original draft, Writing - review & editing. **E. Ferraz:** Writing - review & editing. **A.F. Lourenço:** Writing - review & editing. **P.J. Ferreira:** Writing - review & editing. **M.G. Rasteiro:** Funding acquisition, Writing - review & editing. **J.A.F. Gamelas:** Funding acquisition, Project administration, Writing - review & editing.

Acknowledgments

The present research was supported by the R&D Project "FIL-CNF-New generation of composite films of cellulose nanofibrils with mineral particles as high strength materials with gas barrier properties" (PTDC/QUI-OUT/31884/2017, CENTRO 01-0145-FEDER-031884) and Strategic Research Centre Project UIDB00102/2020, both funded by the Fundação para a Ciência e Tecnologia (FCT). A. F. Lourenço also acknowledges Fundação para a Ciência e Tecnologia for the PhD grant (SFRH/BDE /108095/2015).

Appendix A. Supplementary data

Supplementary material related to this article can be found, in the online version, at doi:https://doi.org/10.1016/j.carbpol.2020.116109.

References

Alves, L., Ferraz, E., Gamelas, J.A.F., 2019. Composites of nanofibrillated cellulose with clay minerals: A review. Advances in Colloid and Interface Science 272, 101994.

Alves, L., Lindman, B., Klotz, B., Böttcher, A., Haake, H.-M., Antunes, F.E., 2014. Controlling the swelling and rheological properties of hydrophobically modified polyacrylic acid nanoparticles: Role of pH, anionic surfactant and electrolyte. Colloids and Surfaces A, Physicochemical and Engineering Aspects 459, 233–239.

Alves, L., Lindman, B., Klotz, B., Böttcher, A., Haake, H.-M., Antunes, F.E., 2015. Rheology of polyacrylate systems depends strongly on architecture. Colloid and Polymer Science 293 (11), 3285–3293.

Calabrese, V., Muñoz-García, J.C., Schmitt, J., da Silva, M.A., Scott, J.L., Angulo, J., … Edler, K.J., 2019. Understanding heat driven gelation of anionic cellulose nanofibrils: Combining saturation transfer difference (STD) NMR, small angle X-ray scattering (SAXS) and rheology. Journal of Colloid and Interface Science 535, 205–213.

Collander, R., 1951. The partition of organic compounds between higher alcohols and water. Acta Chemica Scandinavica 5, 774–780.

da Silva, M.A., Calabrese, V., Schmitt, J., Celebi, D., Scott, J.L., Edler, K.J., 2018. Alcohol induced gelation of TEMPO-oxidized cellulose nanofibril dispersions. Soft Matter 14 (45), 9243–9249.

Dimic-Misic, K., Maloney, T., Gane, P., 2018. Effect of fibril length, aspect ratio and surface charge on ultralow shear-induced structuring in micro and nanofibrillated cellulose aqueous suspensions. Cellulose 25 (1), 117–136.

Fukuzumi, H., Tanaka, R., Saito, T., Isogai, A., 2014. Dispersion stability and aggregation behavior of TEMPO-oxidized cellulose nanofibrils in water as a function of salt addition. Cellulose 21 (3), 1553–1559.

Henriksson, M., Berglund, L.A., Isaksson, P., Lindström, T., Nishino, T., 2008. Cellulose nanopaper structures of high toughness. Biomacromolecules 9 (6), 1579–1585.

Hubbe, M.A., Tayeb, P., Joyce, M., Tyagi, P., Kehoe, M., Dimic-Misic, K., … Pal, L., 2017. Rheology of nanocellulose-rich aqueous suspensions: A review. BioResources 12 (4), 9556–9661.

Joshi, S.C., 2011. Sol-gel behavior of hydroxypropyl methylcellulose (HPMC) in ionic media including drug release. Materials 4 (10), 1861–1905.

Jowkarderis, L., van de Ven, T.G.M., 2015. Rheology of semi-dilute suspensions of carboxylated cellulose nanofibrils. Carbohydrate Polymers 123, 416–423.

Kubáň, V., 1991. Determination of octan-1-ol-water partition coefficients by flow-injection extraction without phase separation. Analytica Chimica Acta 248 (2), 493–499.

Lasseuguette, E., Roux, D., Nishiyama, Y., 2008. Rheological properties of microfibrillar suspension of TEMPO-oxidized pulp. Cellulose 15 (3), 425–433.

López-Rubio, A., Lagaron, J.M., Ankerfors, M., Lindström, T., Nordqvist, D., Mattozzi, A., … Hedenqvist, M.S., 2007. Enhanced film forming and film properties of amylopectin using micro-fibrillated cellulose. Carbohydrate Polymers 68 (4), 718–727.

Lourenço, A.F., Gamelas, J.A.F., Nunes, T., Amaral, J., Mutjé, P., Ferreira, P.J., 2017. Influence of TEMPO-oxidised cellulose nanofibrils on the properties of filler-containing papers. Cellulose 24 (1), 349–362.

Mautner, A., Hakalahti, M., Rissanen, V., Tammelin, T., 2018. Crucial interfacial features of nanocellulose materials. In: Lee, K.-Y. (Ed.), Nanocellulose and sustainability: Production, properties, applications, and case studies. CRC Press, p. 42.

Mendoza, L., Gunawardhana, T., Batchelor, W., Garnier, G., 2018. Effects of fibre dimension and charge density on nanocellulose gels. Journal of Colloid and Interface Science 525, 119–125.

Moberg, T., Sahlin, K., Yao, K., Geng, S., Westman, G., Zhou, Q., … Rigdahl, M., 2017. Rheological properties of nanocellulose suspensions: Effects of fibril/particle dimensions and surface characteristics. Cellulose 24 (6), 2499–2510.

Mráček, A., Varhaníková, J., Lehocký, M., Gřundělová, L., Pokopcová, A., Velebný, V., 2008. The influence of hofmeister series ions on hyaluronan swelling and viscosity. Molecules 13 (5), 1025–1034.

Nechyporchuk, O., Belgacem, M.N., Pignon, F., 2016. Current progress in rheology of cellulose nanofibril suspensions. Biomacromolecules 17 (7), 2311–2320.

Okur, H.I., Hladílková, J., Rembert, K.B., Cho, Y., Heyda, J., Dzubiella, J., … Jungwirth, P., 2017. Beyond the hofmeister series: Ion-specific ef-

fects on proteins and their biological functions. The Journal of Physical Chemistry B 121 (9), 1997–2014.

Quennouz, N., Hashmi, S.M., Choi, H.S., Kim, J.W., Osuji, C.O., 2016. Rheology of cellulose nanofibrils in the presence of surfactants. Soft Matter 12 (1), 157–164.

Reijenga, J., van Hoof, A., van Loon, A., Teunissen, B., 2013. Development of methods for the determination of pKa values. Analytical Chemistry Insights 8, 53–71.

Saito, T., Kimura, S., Nishiyama, Y., Isogai, A., 2007. Cellulose nanofibers prepared by TEMPO-Mediated oxidation of native cellulose. Biomacromolecules 8 (8), 2485–2491.

Sangster, J., 1989. Octanol-water partition coefficients of simple organic compounds. Journal of Physical and Chemical Reference Data 18 (3), 1111–1229.

Sato, Y., Kusaka, Y., Kobayashi, M., 2017. Charging and aggregation behavior of cellulose nanofibers in aqueous solution. Langmuir 33 (44), 12660–12669.

Schenker, M., Schoelkopf, J., Gane, P., Mangin, P., 2019. Rheology of microfibrillated cellulose (MFC) suspensions: Influence of the degree of fibrillation and residual fibre content on flow and viscoelastic properties. Cellulose 26 (2), 845–860.

Šebenik, U., Krajnc, M., Alič, B., Lapasin, R., 2019. Ageing of aqueous TEMPO-oxidized nanofibrillated cellulose dispersions: A rheological study. Cellulose 26 (2), 917–931.

Turbak, A.F., Snyder, F.W., Sandberg, K.R., 1983. Microfibrillated cellulose, a new cellulose product: Properties, uses, and commercial potential. ITT Rayonier Inc., Shelton, WA.

Vadodaria, S.S., Onyianta, A.J., Sun, D., 2018. High-shear rate rheometry of micro-nanofibrillated cellulose (CMF/CNF) suspensions using rotational rheometer. Cellulose 25 (10), 5535–5552.

Wågberg, L., Decher, G., Norgren, M., Lindström, T., Ankerfors, M., Axnäs, K., 2008. The build-up of polyelectrolyte multilayers of microfibrillated cellulose and cationic polyelectrolytes. Langmuir 24 (3), 784–795.

Xie, H., Du, H., Yang, X., Si, C., 2018. Recent strategies in preparation of cellulose nanocrystals and cellulose nanofibrils derived from raw cellulose materials. International Journal of Polymer Science 2018, 25.